Materials Chemistry and Physics 203 (2018) 293–301

Contents lists available at ScienceDirect

Materials Chemistry and Physics

journal homepage: www.elsevier.com/locate/matchemphys

# Mechanical and thermal properties of a room temperature curing epoxy resin and related hemp fibers reinforced composites using a novel in-situ generated curing agent

Yi-le Xu, Abdul Qadeer Dayo, Jun Wang*, An-ran Wang, Dan Lv, Abdeldjalil Zegaoui, Mehdi Derradji, Wen-bin Liu**

*Research Institute of Composite Materials, College of Materials Science and Chemical Engineering, Harbin Engineering University, Harbin 150001, PR China*

## HIGHLIGHTS

- An epoxy resin system which can cure at room temperature within 3 h was designed.
- Reaction of AA with DDM released the heat to promote curing reaction of epoxy.
- Rapid prototyping epoxy/TF composites were prepared.
- 213% and 233% enhancement in Young's modulus and impact strength, respectively.
- The thermal stability of the composites was also improved after the addition of TF.

## GRAPHICAL ABSTRACT

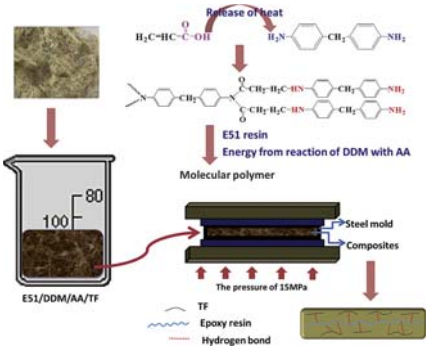


## ARTICLE INFO

*Article history:*
Received 13 June 2017
Received in revised form
28 September 2017
Accepted 2 October 2017
Available online 5 October 2017

*Keywords:*
Self-exothermic hardener
Hemp fibers
Mechanical properties
Thermal properties

## ABSTRACT

A novel self-exothermic curing agent, effectively able to cure the diglycidyl ether of bisphenol-A (E51 epoxy resin) at room temperature, has been synthesized by blending 4, 4'-diaminodiphenylmethane (DDM) and acrylic acid (AA). The chemical structure of prepared curing agent was characterized by $^{1}$H nuclear magnetic resonance ($^{1}$H NMR) and Fourier transform infrared (FTIR). The curing behavior of epoxy with synthesized room temperature hardener was studied by differential scanning calorimetry (DSC) and FTIR. Results confirmed that the curing reaction was completed in only 3 h, which can be attributed to the high reactivity of the acryl amide groups with epoxy and high heat release from DDM and AA reaction. The 5 wt% NaOH treated short hemp fibers (TF) were sandwiched in room temperature curing epoxy resin to obtain rapid prototyping high performance composites. The effects of fiber content on the mechanical properties of composites were studied in terms of tensile, flexural, and impact load. The tensile strength of the composites was increased with the increase of the TF content, and the elongation at break was decreased. Compared with the cured neat epoxy resin, an increase of about 233% in impact strength, 52% in flexural modulus, and 213% in Young's modulus were recorded for the cured composite having 7.5 wt% TF content. We used dynamic mechanical analyzer (DMA) and thermogravimetric analysis (TGA) to study the effect of fiber content on the thermal properties of composites. The scanning electron microscope (SEM) revealed excellent adhesion between TF and epoxy resin cured at room temperature.



* Corresponding author.
** Corresponding author.
*E-mail addresses:* wj6267@sina.com (J. Wang), wjlwb@163.com (W.-b. Liu).

https://doi.org/10.1016/j.matchemphys.2017.10.004
0254-0584/

## 1. Introduction

Epoxy thermosetting resins have received considerable attention by industries because of their favorable mechanical properties, high adhesive strength, low shrinkage on curing, and excellent resistance against chemicals/weather. These excellent properties increased the application of epoxy resins in the fields of adhesives, packaging for electronic devices, insulation, coatings, composites, flooring, and water proofing [1–4]. Epoxy resins are cured in the presence of a curing agent to form the cross-linking structure. Aliphatic amines have several advantages such as high reaction activity, low melting temperature, low viscosity, and general applicability, the key properties for room temperature cure adhesives and coatings. However, the higher volatility, strong sensitization, quick carbonization in the air, and very strict stoichiometric relation against epoxy are their major disadvantages, which restrict their applications in certain fields [4]. The epoxies cured with aromatic amine hardeners showed excellent properties as compared to the aliphatic amine hardeners, however, high polymerization enthalpy, curing temperature, and melting point are the associated drawbacks of aromatic amine hardeners [5,6]. The most commonly used and reported aromatic amine curing agents include 4,4'-diaminodiphenylmethane (DDM) [7–11], 1,3-diaminobenzene [12,13], and 4,4'-diaminodiphenylsulfone (DDS) [14–19]. Dendrimer hardeners have several advantages over traditional amine-based hardeners like lower toxicity, low volatility, and high compatibility with epoxies [20,21], however, the synthesis of dendrimers is complex [22].

Since the start of 21st century, natural fibers (NF) including hemp, jute, kenaf, sisal, banana, oil palm, flax, etc. have attracted more attention as reinforcements in the polymer material. NF have various advantages of eco-friendly, renewable, low density, cost effective, especially when compared to synthetic fiber. In addition, the NF have the advantages of an easy processability, no skin irritation, high mechanical properties, high aspect ratio (L/D), and high insulating and thermal properties, which broaden their usage in different applications [23–26]. Hemp fibers were reported as fillers for various polymer matrices such as epoxies [27–30], polybenzoxazines [31,32], poly(lactic acid) [33,34], starch acetate [35], and vinyl ester [36].

In the current study, a simple synthesis procedure for room temperature curing agent was designed by using the AA as DDM modifier and the chemical structure of curing agent was analyzed by $^1$H NMR. The curing behavior of epoxy resin with the prepared self-exothermic hardener was characterized by FTIR and DSC. Moreover, epoxy resins were reinforced using different amounts of alkali treated hemp fibers (TF) and cured by the prepared curing agent. The effects of the fiber content on the mechanical and thermal properties of the prepared composites were analyzed.

## 2. Experimental

### 2.1. Materials

The epoxy resin (E51) was kindly provided by Jiangxi Huacui Advanced Materials Co. Ltd. (China). The DDM hardener was purchased from Tianjin Kernel Chemical Reagent Co. Ltd. (China). The acrylic acid (AA) was procured from Shanghai Jingchun Reagent Co. Ltd. (China). Short natural hemp fibers (SHF) were kindly donated by Daqing Branch of Heilongjiang Academy of Sciences, Daqing. Ethanol, cyclohexane and sodium hydroxide (NaOH) were procured from Shanghai Jingchun Reagent Co., Ltd., China.

### 2.2. Preparation of composites

The SHF were treated by an alkaline treatment process for the good fiber-resin interfacial adhesion. First of all, washing cycle (i.e. with water, ethanol/cyclohexane (1:1, V/V), and water) was performed on the SHF, for the removal of attached physical and chemical impurities. Afterward, the washed SHF were soaked for 6 h under ambient conditions in a sodium hydroxide solution (5 wt %). Then, the fibers were neutralized by washing with water and acetic acid solution (1 wt%), vacuum dried for overnight at 60 °C, and stored in an air tight pot.

The DDM was mixed with E51 epoxy resin at 60 °C and stirred uniformly. Then an appropriate amount of TF was added into the mixture and cooled down to room temperature. Finally, a certain amount of AA (DDM and AA with molar ratio 1:2) was added to the mixture and stirred uniformly. The composite blends were poured into steel molds having the required dimensions for the test specimens and pressed at 15 MPa pressure for 3 h.

### 2.3. Characterization

The Perkin Elmer Spectrum 100 spectrometer was used to record the FTIR spectra in the range of 4000–450 $cm^{-1}$. FTIR spectra were obtained at 4 $cm^{-1}$ after averaging four (04) scans by casting a thin film on a KBr plate for samples. $^1$H NMR spectra were obtained on a Bruker AVANCE-500 NMR spectrometer with tetramethylsilane (TMS) as an internal standard and $CDCl_3$ was used as the solvent. The average number of transients for $^1$H NMR spectroscopy was 16. DSC was performed under the flow of nitrogen (50 mL/min) on Q200, TA Instruments (USA) at a heating rate of 20 °C/min. The thermal stability of the cured samples was studied from 50 °C to 820 °C under 50 mL/min nitrogen purging. The Q50, TA Instruments (USA), was used at 20 °C/min heating rate. The thermomechanical properties of cured samples were tested on the DMA Q800, TA Instruments (USA). The 30 × 10 × 2 $mm^3$ rectangular sample was loaded under a nitrogen atmosphere in single cantilever mode at 3 °C/min heating ramp and 1 Hz frequency. The specimen with dimensions 50 × 10 × 2 $mm^3$ were tested at 1 mm/min crosshead speed on Instron 5569 instrument for tensile and flexural properties. The Izod impact tests were conducted on IT503 impact-resistance, Tinius-Olsen China, whereas ASTM D256-2010 was followed for evaluating impact resistance of composites. SEM micrographs of gold sputtered fracture surfaces were taken on an electron microscope CamScan MX2600FE, Oxford Instruments, UK, at acceleration voltage of 20 kV using secondary electron detector and a working distance about 35 mm.

## 3. Results and discussion

### 3.1. Synthesis and characterization of room temperature hardener

The reaction of AA with DDM and curing reaction of epoxy resin with the prepared hardener (AA + DDM) at room temperature are shown in Schemes 1 and 2, respectively. The chemical structures of the neat DDM and the prepared curing agent were characterized by $^1$H NMR (Fig. 1). The DDM (curve *a*) indicates that the protons of the primary amine at 3.52 ppm(1), the protons of Ar-$CH_2$-Ar at 3.76 ppm (3), and the protons of phenyl rings at 6.59 and 6.95 ppm (2). After 5 min of mixing of the AA in DDM (curve *b*), the primary amine proton peak at 3.52 ppm disappeared and a new peak attributed the proton acrylamide at 8.51 ppm (1′) was observed. Moreover, the protons of $CH_2$=CH- in the range of 5.93–6.16 ppm (4′) were also observed. The exothermic reaction of DDM and AA produced acrylamide. The produced acrylamide reacted with DDM via Michael addition reaction [4,37]. After 1.5 h of the AA blending

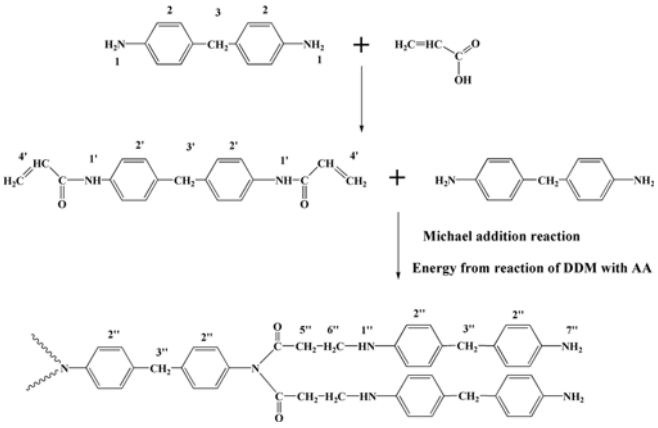


**Scheme 1.** The chemical structure and reaction route of curing agent.

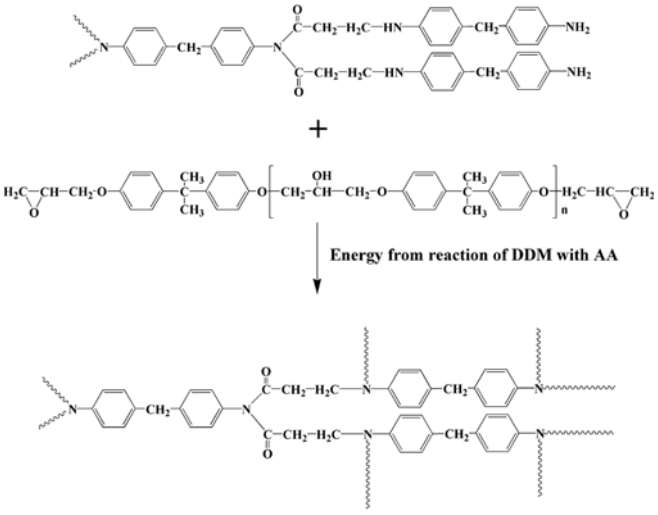


**Scheme 2.** The curing reaction of epoxy resin with hardener.

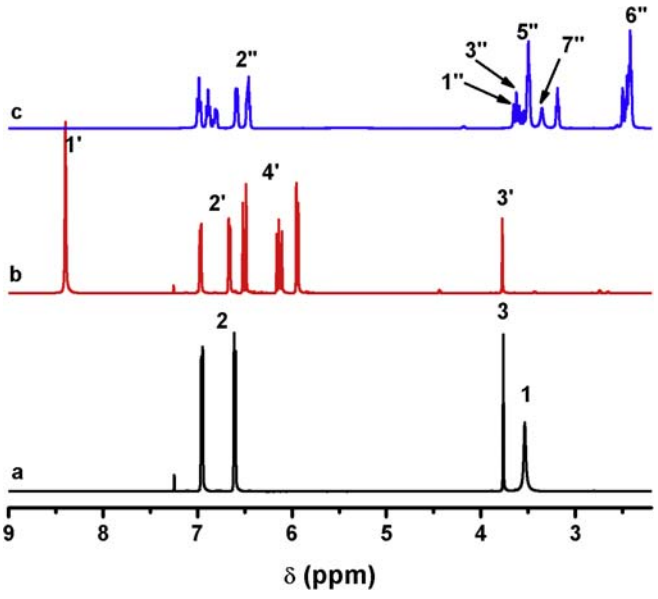


**Fig. 1.** The chemical structure of neat DDM (a), and blend of AA and DDM, after 5 min (b) and 1.5 h (c).

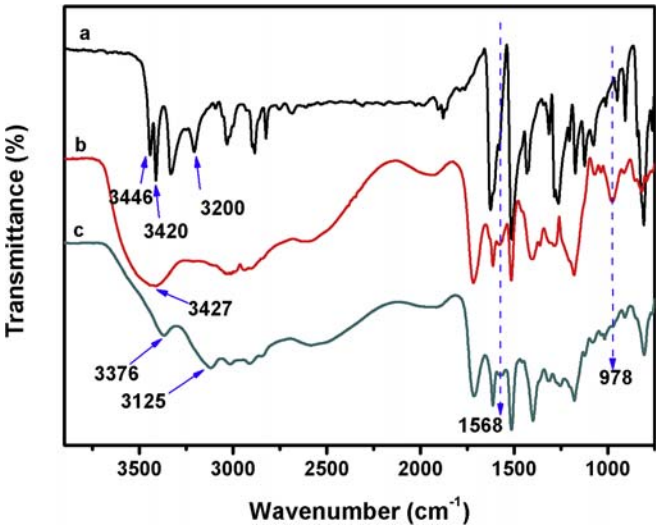


**Fig. 2.** FTIR spectra of neat DDM (a), and blend of AA and DDM for 5 min (b), 1.5 h (c).

with DDM (curve *c*), the $CH_2$=CH- proton peaks at 5.93–6.16 ppm and the acrylamide proton peak at 8.51 ppm disappeared. In addition, new peaks at 6.42–6.62 ppm (2″) attributed to the protons of phenyl ring were observed, which confirms that the Michael addition reaction of acrylamide with unreacted DDM occurred. The two triple peaks at 2.41 ppm (5″) and 3.49 ppm (6″) were assigned to the protons of two methylene groups formed by the Michael addition reaction of vinyl groups. The new single peak at 3.65 ppm (1″) can be attributed to the proton of Ar-NH-alk and the single wide peak at 3.35 ppm (7″) to Ar-$NH_2$.

The FTIR spectra of the DDM and the prepared room temperature curing agent are described in Fig. 2. The DDM (curve *a*) showed the vibration of primary amine peaks at 3446 and 3420 $cm^{-1}$. The 3230 $cm^{-1}$ peak represents the combined peak of aromatic primary amine. After 5 min of blending the AA with DDM (curve *b*), the primary amine peaks at 3446 and 3420 $cm^{-1}$ disappeared, while two new vibration peaks representing the acrylamide were observed at 3427 and 1568 $cm^{-1}$, which confirms the formation of acrylamide from the reaction of the AA with DDM. In addition, a new peak at 978 $cm^{-1}$ attributed to the vibration of $CH_2$=CH- was observed. After 1.5 h of mixing the AA with DDM (curve *c*), the peak at 978 $cm^{-1}$ disappeared and a new combined peak of aromatic primary amine at 3125 $cm^{-1}$ was observed, this suggests that the Michael addition reaction of acrylamide with unreacted DDM occurred. The peaks at 3376 and 1568 $cm^{-1}$ explained the presence of acrylamide in the prepared curing agent.

### 3.2. Curing behavior of room temperature curing epoxy resin

The curing behavior of room temperature curing epoxy resin was characterized by FTIR and DSC, and the produced curves are displayed in Figs. 3and 4. In the epoxy/DDM system (curve *a*), two peaks at 3456 and 3360 $cm^{-1}$ correspond to the vibration of primary amine of DDM. The 3230 $cm^{-1}$ peak represents the combined peak of aromatic primary amine and 915 $cm^{-1}$ peak is related to the vibration of the epoxy group of E51 resin. When AA was added into blends (curve *b*), the peaks of primary amine of DDM at 3456, 3360 and 3230 $cm^{-1}$ were not strong, which indicated the absence of the primary amine as shown in FTIR spectrum. After curing at room temperature for 1.5 h (curve *c*), the peaks of the typical primary amine at 3456 and 3230 $cm^{-1}$ disappeared, which indicated the primary amine of DDM had reacted. However, the peak at

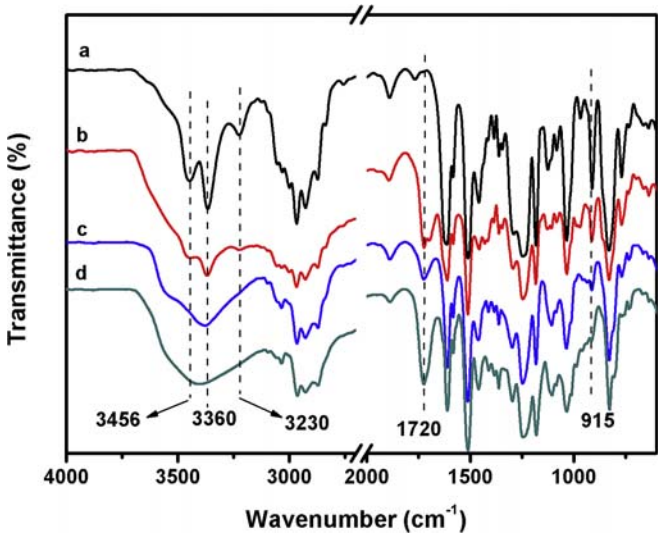


**Fig. 3.** The FTIR spectra of epoxy resin with DDM (a), and after 0 h (b), 1.5 h (c), and 3 h (d) of blending AA in epoxy/DDM.

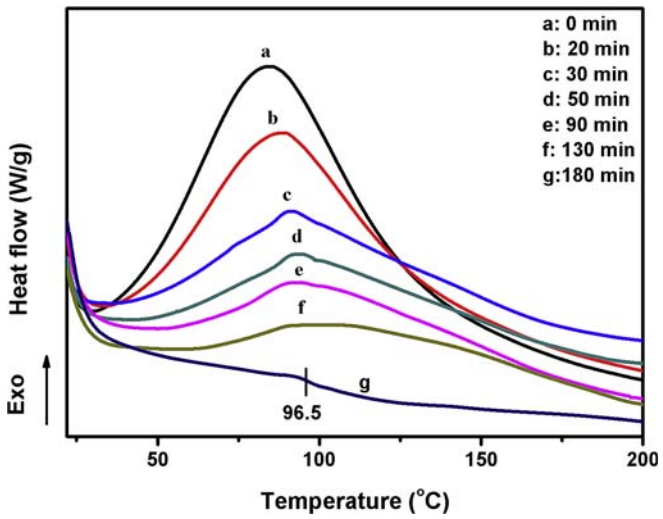


**Fig. 4.** DSC thermograms of epoxy resins at different curing stage.

3360 $cm^{-1}$ did not disappear, suggesting the acrylamide was produced during curing. In addition, the vibration of the epoxy group at 915 $cm^{-1}$ was weakened, suggesting that the curing reaction of epoxy resin with acrylamide was initiated. Subsequently, after curing for 3 h (curve *d*), the peaks at 3360 and 915 $cm^{-1}$ representing the acrylamide and epoxy, respectively, completely disappeared, indicating the completion of curing reaction.

The DSC thermograms of epoxy resins, shown in Fig. 4, indicated that the curing peak gradually weakened and moved towards high temperatures by increasing the curing time. After curing at room temperature for 3 h, the exothermic peak completely disappeared. In addition, the presence of the glass transition on the DSC curve of the cured sample further confirmed that the efficiency of the adopted curing program. The DSC parameters shown in Table 1 indicated that curing reaction enthalpy ($\Delta H$) gradually decreased from 300 to 0 J/g as the curing time proceeds from 0 to 3 h, respectively. In addition, the decline in ($\Delta H$) was high prior to 2 h of curing time, and became slow during 2–3 h. This indicates that the high viscosity of the epoxy system can reduce the movement of chain segments and curing reaction. Moreover, the onset curing temperature and temperature of curing increased from 29 to 50 °C and from 84 to 97 °C, respectively, as the curing time goes on. This can be related to the higher energy demand of epoxy system with the increase of curing degree for the completion of curing reaction.

### 3.3. FTIR of SHF and TF

Since SHF contains hemicellulose, pectin and lignin [31], these substances could be decomposed in acidic media. SHF in the epoxy resin system would be decomposed, resulting in poor performance of composites. Therefore, SHF were treated with NaOH solution to remove these components. The FTIR spectra of SHF and TF are shown in Fig. 5. As compared to the SHF FTIR spectrum, the peak at 1638 $cm^{-1}$, attributed to carbonyl groups of pectin and hemicellulose in fibers, disappeared and the weak peak at 660 $cm^{-1}$ representing the bending peak of carboxylic acid in the pectin almost disappeared as well, which indicates that the pectin and hemicellulose were removed to a great extent by treating with alkali. Moreover, it can be seen that the C-O-C peaks (1260 and 1102 $cm^{-1}$), OH peaks (3432 $cm^{-1}$), CH peaks (2920 $cm^{-1}$) and $CH_2$ symmetric bending peaks (1388 $cm^{-1}$) weakened, which demonstrates partially removed pectin, hemicellulose, and lignin from SHF.

### 3.4. Curing behavior of composites

The FTIR spectra of the epoxy resin/TF composites at different curing stages are given in Fig. 6 and the FTIR spectra of the cured epoxy resin and composites are shown in Fig. 7. It can be seen (Fig. 6) that peak shifts are similar to the shifts of the pure epoxy system (Fig. 7). However, compared with the pure cured epoxy resin in Fig. 7, the hydroxyl peak (3417 $cm^{-1}$) on the FTIR spectrum of the composite is wider, which can be attributed to a larger number of hydrogen bonds formed between hydroxyl groups of the fibers and hydroxyl groups generated in the curing reaction of epoxy resin.

### 3.5. Mechanical properties

The effects of the fiber content on the mechanical properties of the resulting composites were investigated by the tensile, bending

**Table 1**
The onset temperature of curing, temperature of curing reaction and enthalpy of curing of epoxy resin at different curing stages as determined by DSC.

| Curing time (Min) | Onset temperature of curing (°C) | Temperature of curing reaction (°C) | Enthalpy of curing (J/g) |
|---|---|---|---|
| 0 | 29 | 84 | 300 |
| 20 | 30 | 88 | 225 |
| 30 | 29 | 92 | 137 |
| 50 | 35 | 93 | 110 |
| 90 | 40 | 93 | 77 |
| 130 | 50 | 97 | 66 |
| 180 | – | – | 0 |

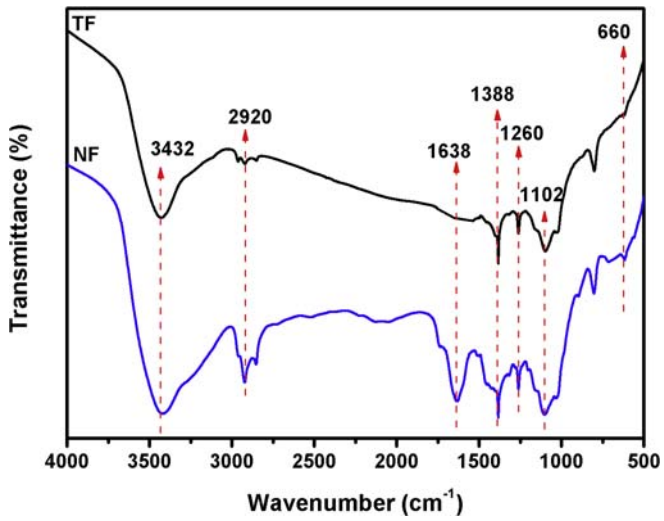


**Fig. 5.** The FTIR spectra of SHF and TF.

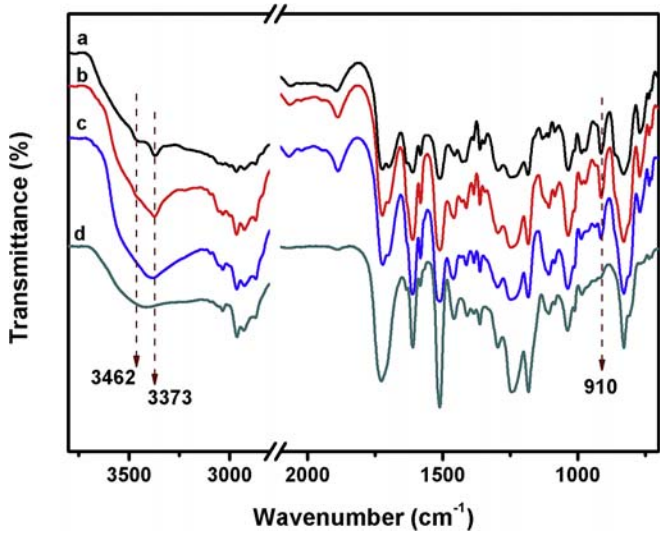


**Fig. 6.** The FTIR spectra of epoxy resin/TF composites at different curing stage, 0 h (a), 1 h (b), 2 h (c), and 3 h (d).

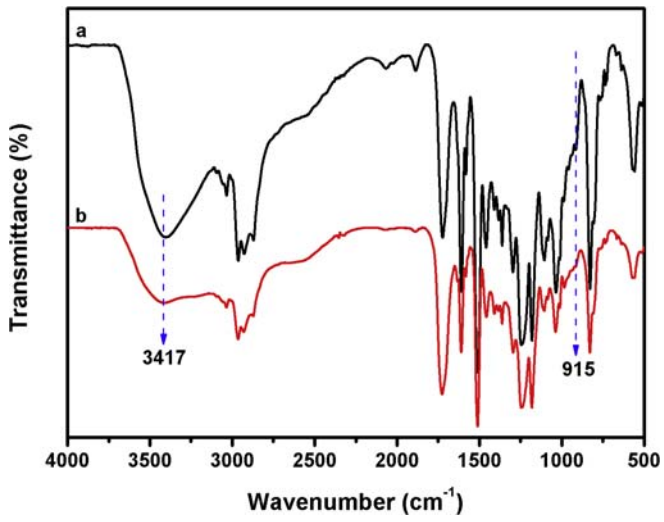


**Fig. 7.** The FTIR curves of the cured pure epoxy resin (a) and TF composite (b).

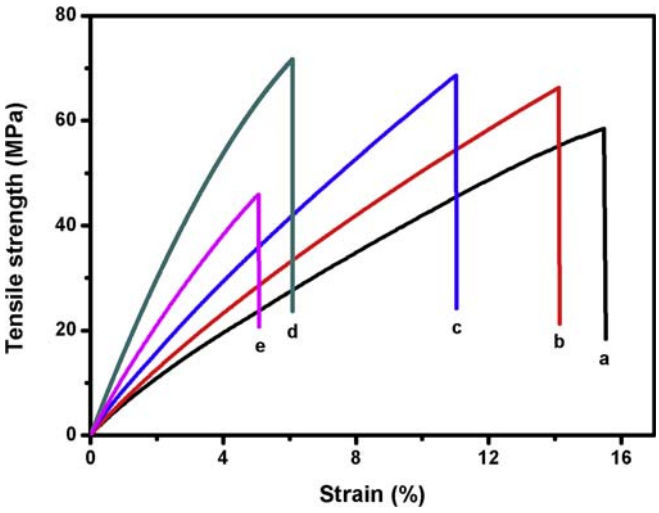


**Fig. 8.** The stress-strain curves of composites at 0% (a), 2.5% (b), 5% (c), 7.5% (d), and 10 wt% (e) TF loading.

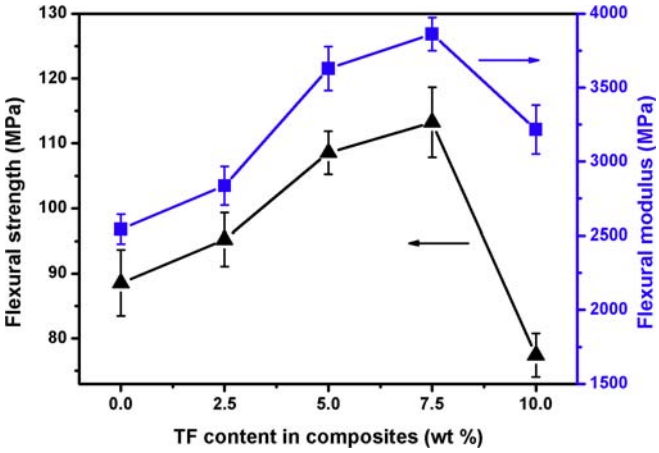


**Fig. 9.** The effects of TF wt% loading on flexural properties of composites.

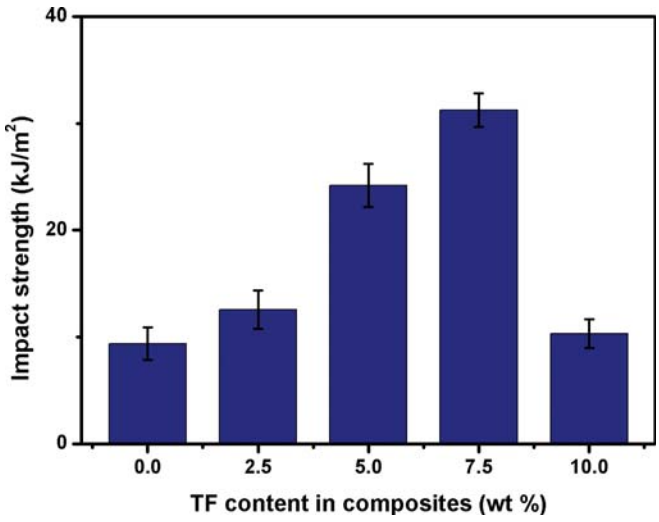


**Fig. 10.** The effects of TF wt% loading on the impact strength of composites.

**Table 2**
The mechanical properties of room temperature curing epoxy resin and related composites.

| Sample | Tensile properties | | | Flexural properties | | Impact strength (kJ/m$^2$) |
|---|---|---|---|---|---|---|
| | Strength (MPa) | Modulus (MPa) | Elongation (%) | Strength (MPa) | Modulus (MPa) | |
| Epoxy | 58.51 | 377.97 | 15.48 | 88.56 | 2544 | 9.37 |
| Epoxy/TF2.5 | 66.29 | 469.47 | 14.12 | 95.2 | 2836 | 12.56 |
| Epoxy/TF5 | 68.69 | 623.32 | 11.02 | 108.56 | 3629 | 24.18 |
| Epoxy/TF7.5 | 71.72 | 1181.55 | 6.07 | 113.26 | 3862 | 31.24 |
| Epoxy/TF10 | 45.97 | 908.49 | 5.06 | 77.43 | 3216 | 10.31 |

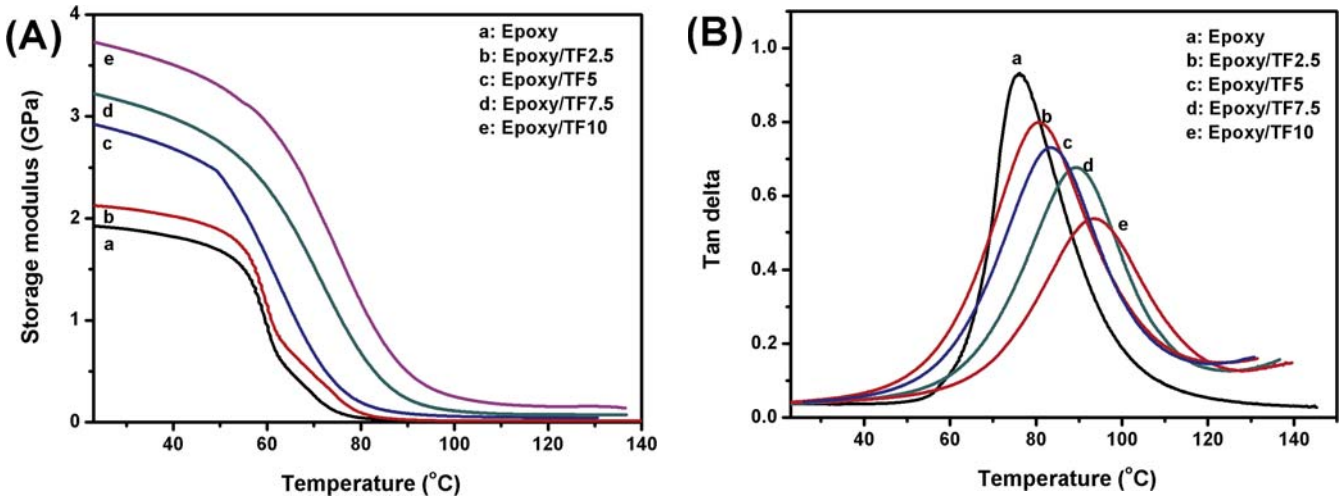


**Fig. 11.** The thermomechanical properties of TF filled composites, storage modulus (A) and *tan delta* (B).

**Table 3**
DMA and TGA results of room temperature curing epoxy resin and related composites.

| Sample | DMA | | TGA | | |
|---|---|---|---|---|---|
| | Storage modulus (MPa) | $T_g$ (°C) | $T_{5\%}$ (°C) | $T_{10\%}$ (°C) | $Y_c$ (at 800 °C) (%) |
| Epoxy | 1927 | 76.1 | 194.5 | 246.7 | 17.84 |
| Epoxy/TF2.5 | 2126 | 80.1 | 197.3 | 253.8 | 12.84 |
| Epoxy/TF5 | 2925 | 85.2 | 199.9 | 264.4 | 13.94 |
| Epoxy/TF7.5 | 3225 | 90.1 | 207.0 | 277.0 | 18.97 |
| Epoxy/TF10 | 3762 | 93.5 | 208.3 | 319.2 | 14.89 |

and impact tests as shown in Figs. 8–10 and the corresponding data were summarized in Table 2. From the tensile stress-strain curves, it can be observed that the elongation at break decreased in the system Epoxy/TF0 to Epoxy/TF7.5. Meanwhile, the tensile strength increased from 58.51 MPa to 71.72 MPa with 23% improvement. Moreover, in contrast with the system Epoxy/TF0, Young's modulus of other composites had been greatly improved. The Epoxy/TF7.5 system exhibited the maximum modulus, resulting in an increase of 213%, which indicates that a large amount of hydrogen bonds were generated between hydroxyl groups of the fibers and matrix, causing the high adhesion in composites. However, the tensile, flexural and impact properties of Epoxy/TF10 system decreased.

The flexural strength, modulus and impact strength increased with the increase of fiber content up to 7.5% with improvements of 28%, 36% and 233%, respectively (Figs. 9 and 10). Compared with the pure epoxy resin, the improvements in tensile and bending strength of the composites are relatively low, which indicated that the TF cannot bear too much load in the matrix. However, the impact strength increased by more than 2 times, mainly due to the formation of hydrogen bonds between the fiber and resin, which could disperse the internal stress generated by the imposed load, making the fibers play the role of absorption of impact energy.

### 3.6. Dynamic mechanical analysis (DMA)

The DMA was used to evaluate the thermomechanical behavior of the room temperature cured epoxy resin and its composites. The variation in the storage modulus ($G'$) and *tan delta* as a function of temperature for the cured epoxy and the related composites are depicted in Fig. 11, and parameters are listed in Table 3. The storage modulus reflects the deformation of the material under a certain load. It can be seen that the storage modulus increased with the increase of the fiber content from 1927 MPa for the neat epoxy to 3762 MPa for the composite with 10 wt% TF (Table 3). The Epoxy/TF10 system has the maximum modulus value, resulting in an increase of 95% compared with the Epoxy system. The main reason is that the number of hydrogen bonds between the fiber and the matrix increased, reducing the segmental motion in the composite material, thus enhancing the storage modulus of the composite materials.

The damping factor (*tan delta*) represents the adhesion between the filler and the matrix in the composite [38]. It can be seen from

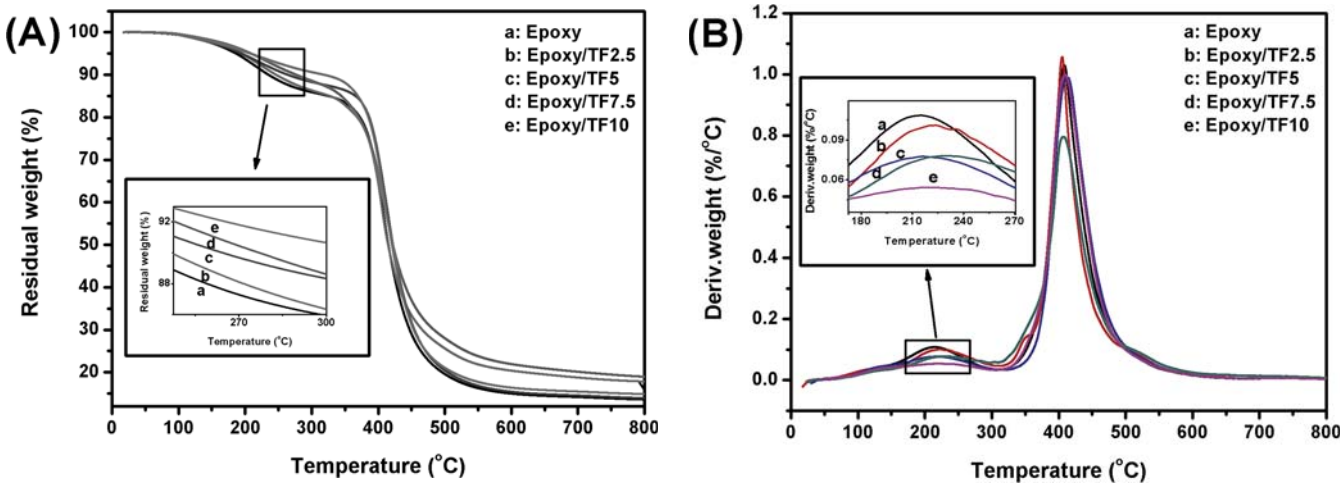


**Fig. 12.** TGA (A) and DTG (B) curves of cured epoxy resin and composites.

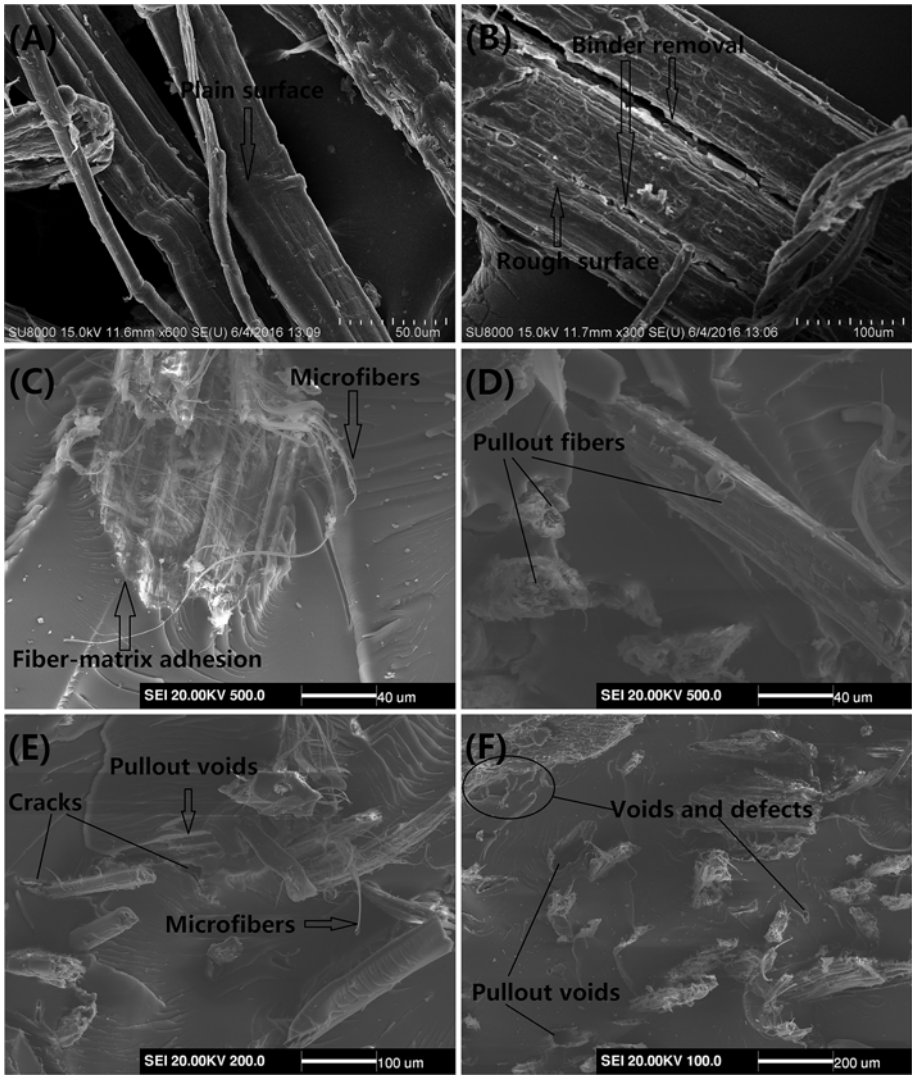


**Fig. 13.** The SEM micrographs of SHF (A) and TF (B), and bending fracture surface of composites with 2.5–10 wt% TF loading(C-F).

*tan delta* curves in Fig. 11(B) that the curve peak value decreased and became wider as the fiber content increased. The decrease in *tan delta* peak value represents a stronger adhesion between the fibers and the matrix in the composites. Moreover, we also

observed that the glass transition temperature ($T_g$) of the material increased with the content of reinforcing fibers, indicating the increased rigidity of polymer chains [39].

### 3.7. Thermogravimetric analysis (TGA)

The thermal stability of cured epoxy and composites was studied by TGA (Fig. 12, Table 3). It can be seen from Fig. 12(A) that the thermal stability of composites was improved by fibers content in epoxy resin. The decomposition temperatures at 5% and 10% mass loss ($T_{5\%}$ and $T_{10\%}$) of the composites were slightly improved from 194.5 °C to 208.3 °C and from 246.7 °C to 319.2 °C with the increase of the fibers content up to 10 wt% (Table 3). The thermal stabilization effect of treated hemp fibers was ascribed to excellent heat resistance of TF and a large number of hydrogen bonds between TF and epoxy matrix as determined by FTIR (Fig. 7).

The DTG curves of cured epoxy and composites (Fig. 12(B)) display two mass loss processes. The alkyl chains produced from Michael addition reaction can be easily decomposed at a lower temperature, causing the first weight loss process at about 200 °C [20,21]. In addition, by increasing the fiber content in the composite, the alkyl chain content in the system decreased, resulting that the low temperature weight loss peak weakened. The mass loss process at about 400 °C is assigned to the decomposition of the epoxy resin. Compared to the pure epoxy resin, the mass loss of composites gradually decreased due to the higher thermal stability of the TF indicating a reinforcement effect of TF.

### 3.8. Morphology

The surface morphology of fibers and fiber-matrix interface adhesion of composites were studied by SEM (Fig. 13). It can be clearly seen from Fig. 13(A) that the SHF had a relatively smooth surface, without any defects and holes. On the other hand, the surface of the alkali treated fibers became rough and some free spaces were also observed on the fiber surface, which is ascribed to removal of hemicellulose, pectin and lignin from SHF during alkali treatment. The resulting voids and rough surfaces can accommodate the epoxy resin, resulting in excellent adhesion between the fibers and matrix, thereby improving the performance of the composites. From Fig. 13(C)–(F), it can be seen that the fiber diameter is about 40–100 μm. From Fig. 13(C), there was no defect and bubble on the fracture surface and plenty of microfibers were observed, showing an excellent interface between the resin and the fiber. In Fig. 13(E), voids formed by fibers pullout from matrix were found. We can also observe cracks on the edges of these holes. This is because the adhesive stress between the matrix and fiber caused the resin to crack when the fiber came out of the matrix. These observations can prove that the fibers were effectively bonded to the epoxy matrix. In addition from Fig. 13(F), some bubbles and defects were found on the interface between fiber and resin. This is because of the fibers' agglomeration occurred on the high fiber content, resulting in the low adhesion between the fibers and producing bubbles and defects.

## 4. Conclusions

A new kind of epoxy resin system which can be quickly cured at room temperature was designed. The structure of room temperature curing agent was characterized by FTIR and $^1$H NMR. The course of reaction of the system at room temperature curing was studied by FTIR and DSC analysis. Both studies confirmed that the epoxy resin was completely cured within 3 h at room temperature. Moreover, SHF were treated with the alkaline solution and TF were reinforced in the epoxy system cured at room temperature. Hydrogen bonding was confirmed between the resin and TF from the FTIR spectra of composites. Mechanical properties were improved after the addition of TF in the epoxy resin and reached its maximum values at only 7.5 wt% loading. Thermal stabilities of the TF composites were also improved as the reinforcement of TF increased. The morphology studies revealed that the adhesion of epoxy resin with TF was good due to the existence of hydrogen bonds.

## Acknowledgements

The financial support from the National Natural Science Foundation of China (Project No. 51773048), Natural Science Foundation of Heilongjiang Province (Project No. E2016025), and Fundamental Research Funds for the Central Universities (Project No. HEUCFP201724 and HEUCFP201791) are greatly appreciated by the authors.

## References

[1] H. Lee, K. Neville, Letters - "book review - handbook of epoxy resins", Ind. Eng. Chem. 59 (1967) 16–17.
[2] D. Wu, L. Wu, J. Wang, Y. Sun, M. Zhang, Effect of epoxy resin on the thermal behaviors and viscoelastic properties of poly(phenylene sulfide), Mater. Chem. Phys. 128 (2011) 274–282.
[3] B. De, N. Karak, A room temperature cured low dielectric hyperbranched epoxy adhesive with high mechanical strength, J. Chem. Sci. 126 (2014) 587–595.
[4] J. Wan, C. Li, Z.-Y. Bu, C.-J. Xu, B.-G. Li, H. Fan, A comparative study of epoxy resin cured with a linear diamine and a branched polyamine, Chem. Eng. J. 188 (2012) 160–172.
[5] L. Yao, J. Deng, B.-j. Qu, W.-f. Shi, Cure kinetics of DGEBA with hyperbranched poly (3-hydroxyphenyl) phosphate as curing agent studied by non-isothermal DSC1, Chem. Res. Chin. Univ. 22 (2006) 118–122.
[6] S.R. Patel, R.G. Patel, Comparative studies on the curing kinetics and thermal stability of tetrafunctional epoxy resins using various amines as curing agents, J. Therm. Anal. 39 (1993) 229–238.
[7] S.V. Levchik, G. Camino, M.P. Luda, L. Costa, G. Muller, B. Costes, Epoxy resins cured with aminophenylmethylphosphine oxide—II. Mechanism of thermal decomposition, Polym. Degrad. Stab. 60 (1998) 169–183.
[8] M. Blanco, M.A. Corcuera, C.C. Riccardi, I. Mondragon, Mechanistic kinetic model of an epoxy resin cured with a mixture of amines of different functionalities, Polymer 46 (2005) 7989–8000.
[9] L.A. Mercado, M. Galià, J.A. Reina, Silicon-containing flame retardant epoxy resins: synthesis, characterization and properties, Polym. Degrad. Stab. 91 (2006) 2588–2594.
[10] C. Ortiz, R. Kim, E. Rodighiero, C.K. Ober, E.J. Kramer, Deformation of a polydomain, liquid crystalline epoxy-based thermoset, Macromolecules 31 (1998) 4074–4088.
[11] C.C. Su, E.M. Woo, Chemical interactions in blends of bisphenol A polycarbonate with tetraglycidyl-4,4'-diaminodiphenylmethane epoxy, Macromolecules 28 (1995) 6779–6786.
[12] T. Dyakonov, Y. Chen, K. Holland, J. Drbohlav, D. Burns, D.V. Velde, L. Seib, E.J. Soloski, J. Kuhn, P.J. Mann, W.T.K. Stevenson, Thermal analysis of some aromatic amine cured model epoxy resin systems—I: materials synthesis and characterization, cure and post-cure, Polym. Degrad. Stab. 53 (1996) 217–242.
[13] N. Sbirrazzuoli, A. Mititelu-Mija, L. Vincent, C. Alzina, Isoconversional kinetic analysis of stoichiometric and off-stoichiometric epoxy-amine cures, Thermochim. Acta 447 (2006) 167–177.
[14] J. McGroarty, DDS as an epoxy resin hardener, Ind. Eng. Chem. 52 (1960) 17–18.
[15] M. Opalički, J.M. Kenny, L. Nicolais, Cure kinetics of neat and carbon-fiber-reinforced TGDDM/DDS epoxy systems, J. Appl. Polym. Sci. 61 (1996) 1025–1037.
[16] S.-R. Lu, H.-L. Zhang, C.-X. Zhao, X.-Y. Wang, Studies on the properties of a new hybrid materials containing chain-extended urea and SiO2–TiO2 particles, Polymer 46 (2005) 10484–10492.
[17] P. Khurana, A.K. Narula, V. Choudhary, Curing and thermal behavior of diglycidyl ether of bisphenol A in the presence of a mixture of amines, J. Appl. Polym. Sci. 90 (2003) 1739–1747.
[18] B. Schartel, U. Braun, A.I. Balabanovich, J. Artner, M. Ciesielski, M. Döring, R.M. Perez, J.K.W. Sandler, V. Altstädt, Pyrolysis and fire behaviour of epoxy systems containing a novel 9,10-dihydro-9-oxa-10-phosphaphenanthrene-10-oxide-(DOPO) -based diamino hardener, Eur. Polym. J. 44 (2008) 704–715.
[19] H. Ren, J. Sun, B. Wu, Q. Zhou, Synthesis and properties of a phosphorus-containing flame retardant epoxy resin based on bis-phenoxy (3-hydroxy) phenyl phosphine oxide, Polym. Degrad. Stab. 92 (2007) 956–961.
[20] D.-M. Xu, K.-D. Zhang, X.-L. Zhu, Curing of DGEBA epoxy resin by low generation amino-group-terminated dendrimers, J. Appl. Polym. Sci. 101 (2006) 3902–3906.

[21] C. Yiyun, C. Dazhu, F. Rongqiang, H. Pingsheng, Behavior of polyamidoamine dendrimers as curing agents in bis-phenol A epoxy resin systems, Polym. Int. 54 (2005) 495–499.
[22] Y. Cheng, T. Xu, P. He, Polyamidoamine dendrimers as curing agents: the optimum polyamidoamine concentration selected by dynamic torsional vibration method and thermogravimetric analyses, J. Appl. Polym. Sci. 103 (2007) 1430–1434.
[23] M. Prasad Bhuwan, M. Sain Mohini, D.N. Roy, Properties of ball milled thermally treated hemp fibers in an inert atmosphere for potential composite reinforcement, J. Mater. Sci. 40 (2005) 4271–4278.
[24] V.K. Baheti, R. Abbasi, J. Militky, Ball milling of jute fibre wastes to prepare nanocellulose, World J. Eng. 9 (2012) 45–50.
[25] J. Militký, A. Jabbar, Comparative evaluation of fiber treatments on the creep behavior of jute/green epoxy composites, Compos. Part B Eng. 80 (2015) 361–368.
[26] A. Bismarck, I. Aranberri-Askargorta, J. Springer, T. Lampke, B. Wielage, A. Stamboulis, I. Shenderovich, H.-H. Limbach, Surface characterization of flax, hemp and cellulose fibers; Surface properties and the water uptake behavior, Polym. Compos. 23 (2002) 872–894.
[27] D.S. de Vasconcellos, F. Sarasini, F. Touchard, L. Chocinski-Arnault, M. Pucci, C. Santulli, J. Tirillò, S. Iannace, L. Sorrentino, Influence of low velocity impact on fatigue behaviour woven hemp fibre reinforced epoxy composites, Compos. Part B Eng. 66 (2014) 46–57.
[28] D.S. de Vasconcellos, F. Touchard, L. Chocinski-Arnault, Tension–tension fatigue behaviour of woven hemp fibre reinforced epoxy composite: a multi-instrumented damage analysis, Int. J. Fatigue 59 (2014) 159–169.
[29] B.M. Wood, S.R. Coles, S. Maggs, J. Meredith, K. Kirwan, Use of lignin as a compatibiliser in hemp/epoxy composites, Compos. Sci. Technol. 71 (2011) 1804–1810.
[30] C. Guillebaud-Bonnafous, D. Vasconcellos, F. Touchard, L. Chocinski-Arnault, Experimental and numerical investigation of the interface between epoxy matrix and hemp yarn, Compos. Part A Appl. Sci. Manuf. 43 (2012) 2046–2058.
[31] A.Q. Dayo, B.-c. Gao, J. Wang, W.-b. Liu, M. Derradji, A.H. Shah, A.A. Babar, Natural hemp fiber reinforced polybenzoxazine composites: curing behavior, mechanical and thermal properties, Compos. Sci. Technol. 144 (2017) 114–124.
[32] A.Q. Dayo, Y.-l. Xu, A. Zegaoui, A.A. Nizamani, J. Wang, L. Zhang, W.-b. Liu, A.H. Shah, Reinforcement of waste hemp fibres in aromatic diamine-based benzoxazine thermosets for the enhancement of mechanical and thermo-mechanical properties, Plast. Rubber Compos. https://doi.org/10.1080/14658011.2017.1386366.
[33] N. Graupner, Improvement of the mechanical properties of biodegradable hemp fiber reinforced poly(lactic acid) (PLA) composites by the admixture of man-made cellulose fibers, J. Compos. Mater. 43 (2009) 689–702.
[34] R. Hu, J.-K. Lim, Fabrication and mechanical properties of completely biodegradable hemp fiber reinforced polylactic acid composites, J. Compos. Mater. 41 (2007) 1655–1669.
[35] R. Joffe, B. Madsen, K. Nättinen, A. Miettinen, Strength of cellulosic fiber/starch acetate composites with variable fiber and plasticizer content, J. Compos. Mater. 49 (2015) 1007–1017.
[36] G. Francucci, N. Manthey, F. Cardona, T. Aravinthan, Processing and characterization of 100% hemp-based biocomposites obtained by vacuum infusion, J. Compos. Mater. 48 (2014) 1323–1335.
[37] E.J.-C. Amieva, C. Velasco-Santos, A. Martínez-Hernández, J. Rivera-Armenta, A. Mendoza-Martínez, V. Castaño, Composites from chicken feathers quill and recycled polypropylene, J. Compos. Mater. 49 (2015) 275–283.
[38] D. Shanmugam, M. Thiruchitrambalam, Static and dynamic mechanical properties of alkali treated unidirectional continuous Palmyra Palm Leaf Stalk Fiber/jute fiber reinforced hybrid polyester composites, Mater. Des. 50 (2013) 533–542.
[39] H.-D. Kim, H. Ishida, A study on hydrogen-bonded network structure of polybenzoxazines, J. Phys. Chem. A 106 (2002) 3271–3280.